



# Study on Anchorage Failure and Bolting Measures of Roadway in Weak Rock

Enyuan Dong · Weijun Wang

Received: 19 February 2019 / Accepted: 3 September 2019 / Published online: 10 September 2019  
© Springer Nature Switzerland AG 2019

**Abstract** A mechanical model for anchorage and surrounding rock was established against the failure of bolting system, the differential equation of load-transfer was solved and the shape and depth of excavation damaged zone (EDZ) of the surrounding rock was analysed. The results show that to achieve full performance of rockbolts materials and to lengthen its service life, two requirements must be met. One is that the load of rockbolt is no more than its load-bearing capacity. The other one is that the anchorage should be located in stable elastic zone. The shape of EDZ is determined by the magnitude and direction of in-situ stress. Reasonable bolting design should abandon the traditional design of uniform support strength. Rather, should adopt coordinated support and nonuniform support design according to the shape of EDZ in field. Based on the above principles, a new type of combination rockbolt with the effect of high resistance and yield pattern was adopted for the new bolting scheme in the main roadway of Puhe Coal Mine. By analyzing the data

collected in field, it is concluded that the combination rockbolt can solve the problem that appearing pull-out failure of rockbolts and tensile failure of cablebolts.

**Keywords** Bolting failure · Weak mass · EDZ · Coordinated support

## 1 Introduction

Support of roadway in weak rock is always a challenge due to complex geological conditions and the special mechanical properties. Therefore, the methods of raising rockbolt's strength and increasing density of rockbolts installed are simply adopted. However, bolting failure, which will lead to accidents, still occurs (Indraratna and Kaiser 2010). It illustrates that it's not the reason of insufficient support strength, but the lack of understanding to the relationship between bolting failure and the deformation mechanism of surrounding rock. Only blindly increasing the support strength of roadway, it cannot produce a good support effect. In this case, the method may lead to excessive support and increase the support cost (Peila 1994; Anagnostou and Perazzelli 2015).

At present, due to the high cost of field tests, the failure mechanism of anchorage is generally studied by laboratory test and theoretical analysis. Li et al. (2019) conducted a series of tests using a drop mass of

---

E. Dong (✉) · W. Wang  
School of Resource Environment and Safety Engineering,  
Hunan University of Science and Technology,  
Xiangtan 411201, China  
e-mail: dongenyuan1103@126.com

W. Wang  
Hunan Provincial Key Laboratory of Safe Mining  
Techniques of Coal Mines, Hunan University of Science  
and Technology, Xiangtan 411201, China

up to 185 kg from a maximum height of 3 m based on a double shear test system. Tahmasebinia et al. (2018) developed numerical and a novel analytical simulation technique for cablebolt rockbolts to assess their structural behaviour under static and dynamic loading conditions. Yu et al. (2019) analyzed numerically the critical rockbolt embedment length at which yielding or necking occurs together with the friction coefficient at the residual axial stress. Li et al. (2019) experimentally and analytically investigated the behaviour of two different cablebolts, including Sumo and TG using an advanced pull-out testing facility capable of testing the cablebolts under axial loading and constant normal stiffness. Zou and Zhang (2019) investigated the dynamic evolution characteristic of the bond strength at the interface of a rockbolt and a rock mass under an axial tensile load and the mechanical behavior of fully grouted rockbolts in situ considering the non-uniform stress of the surrounding rock along the rockbolts. Teymen and Kılıç (2018) conducted an experimental research considering the only axial forces acting on the fully grouted rockbolts and investigated stress–strain mechanism of the bolt–grout interface.

Farmer (1975) studied the distribution of shear stress on the resin–rock interface through traditional anchor pullout test. Blanco Martín et al. (2013) proposed a method to predict the mechanical characteristics of full-grouted rockbolt. Li et al. (2017) established a constitutive model to predict the displacement characteristics curve of improved rockbolt under full load and different confining pressure. Cai et al. (2015) established the anchorage analysis model of bolt–rock interface under isotropic and uniform stress field conditions, analyzed the distribution of axial force and the characteristics of the coupling and uncoupling of the interface, and analyzed the mechanical mechanism of anchorage based on the elastic–plastic concept and strain softening characteristics of surrounding rock. Li and Stillborg (1999) analyzed the analytic solutions of shear stress of rockbolt under three conditions, which were the tension effect of the rockbolt, the influence of the deformation and cracking of rock on rockbolt respectively.

The failure of the traditional anchorage system mainly includes the breakage failure of rockbolt, the dilatation slip failure of the bolt–grout interface, the dilatation slip failure of the grout–rock interface, the

global failure of anchorage and rock together (You and Zhan 2005; Hyett et al. 1995) (Fig. 1).

The resin–rock interface is the key to the bolting system. The research emphasis should be put on the mechanical properties of the interface (Serrano and Olalla 1999; Kiliç and Celik 2002). The material properties are determined for the selected rockbolt and capsule resin. To some extent, there are certain changes for properties of surrounding rock due to the excavation of roadway (Barton and Shen 2016; Tsang et al. 2005; Wang et al. 2015, 2017). Therefore, studying the damage degree of surrounding rock has an important significance in guiding the correct bolting design.

In this paper, the mechanical model of the resin–rock interface is established to study its influence on bolting. At the same time, the distribution of EDZ of surrounding rock around an excavation was analyzed, the purpose of which is to grasp the correct control mechanism of deformation of surrounding rock to reveal the causes of anchorage failure under the condition of high strength and excessive support. Finally, the anchorage failure of the main roadway in Puhe Coal Mine was analyzed and verified.

## 2 Engineering Background

Puhe Coal Mine locates in Shenyang city, China. The shape of the main roadway is semicircle arch. The roadway lies in the siltstone strata under the floor of coal strata. The roof strata within the range of 7 m are the interbed of mudstone and sandy mudstone, whose characteristic is black, brittle, without bedding. Meanwhile, within the range of 7–27 m, the roof strata is the interbed of siltstone and fine sandstone, whose characteristic is black, compact, and the shell fracture. The floor strata are hosts oil shale and other weak rock

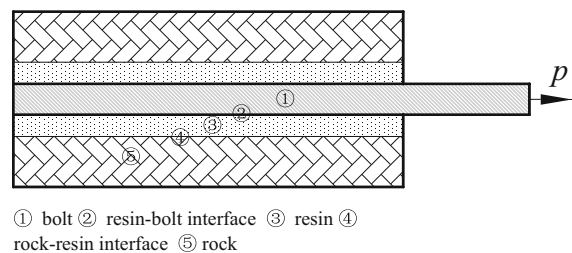


**Fig. 1** Sketch of anchorage failure

mass with expansibility. There is a fracture zone around the roadway, and its displacement is larger after excavation. The mechanical parameters are shown in Table 1.

The roadway adopted the combined support with rockbolt + wire mesh + cablebolt + beam + shotcrete. The cablebolt of  $\Phi 17.8 \times 7000$  mm is twisted with 7 strands of wire rope. A hanging beam of 1.6 m length used for the cablebolts is made of 36U steel. The anchorage agent is made of resin with the specification of  $\Phi 23$  mm  $\times$  500 mm. The wire mesh of 10 m  $\times$  1 m (length  $\times$  width) adopts 10# wire mesh. The shotcrete thickness is 100 mm. The steel ladder of 80 mm width and 2500 mm length is made of round steel of 10 mm diameter. The support cross-section and the inter-row spacing are shown in Fig. 2. After installing the rockbolts and cablebolts of the original support scheme, the rockbolts were often pulled out from anchorage, and the cablebolts were broken easily in local section of the roadway.

By setting monitoring points on the left and right sidewall of three different cross-sections respectively, the depth of excavation damaged zone (EDZ) was observed by multifunctional ultrasonic instrument, as shown in Fig. 3. The principle of ultrasonic method is that, the ultrasonic velocity is different in different medium, the velocity in homogeneous rock is faster than that of in fractured rock. Therefore, the fractured zone can be predicted according to the ultrasonic velocity. The position of the monitoring points and the ultrasonic velocity collected are shown in Figs. 4, 5 and 6. The monitoring points of displacement were installed by drilling boreholes at the roof. And the monitoring points of EDZ were fixed to the rock surface on the sidewall of roadway.

Therefore, the depth of EDZ was about 2.3–2.7 m according to the distribution of compressive wave. From the field, it was found that the rockbolts were

mainly pulled out from the anchorage with the deformation of surrounding rock, and were rarely broken.

The displacements of surrounding rock at different depths and different time were measured using displacement gauge installed in three different roof positions. The locations of the monitoring points and displacement gauge are shown in Fig. 4. The monitoring instruments are shown in Fig. 7. Figures 8, 9 and 10 show displacement of monitoring points.

It can be seen from the displacement monitoring chart that the displacement of the roof is about 400 mm, no synchronous sinking occurred within the scope of monitoring, and there is a bed separation, whose maximum separation location is between 2 and 4 m. The maximum elongation of cablebolt is 3%, while in field only 2%. The maximum elongation of cablebolt used by the roadway is about 140 mm, which is much lower than the displacement of roof, leading to the breaking failure of a large number of cablebolts.

### 3 Analysis of Bolting Failure

The objective of bolting is to control the deformation of surrounding rock by providing enough anchoring force, which depends on the performance of anchorage. The failure always occurs from the weakest point. The rockbolt is broken if its tensile strength reaches to critical tensile strength, the case in which shows that the rockbolt plays a better supporting effect. When the bonding interface failure occurs, some of the material performance of rockbolt has been wasted. Therefore, under the premise of avoiding the failure of the bonding interface, it is necessary to take some measures to prevent the breakage of rockbolt or to extend its lifetime as far as possible.

**Table 1** Mechanical parameters of rock

Rock description	Young's modulus/Gpa	Compression strength/Mpa	Tension strength/Mpa	Cohesion/Mpa	Poisson's ratio
Fine sandstone	53.8	34.65	1.73	2.56	0.28
Sandy mudstone	22.96	14.21	1.55	1.73	0.25
Mudstone	10.35	15.28	1.13	1.84	0.32
Shale sandstone	32.00	29.56	1.35	2.43	0.22

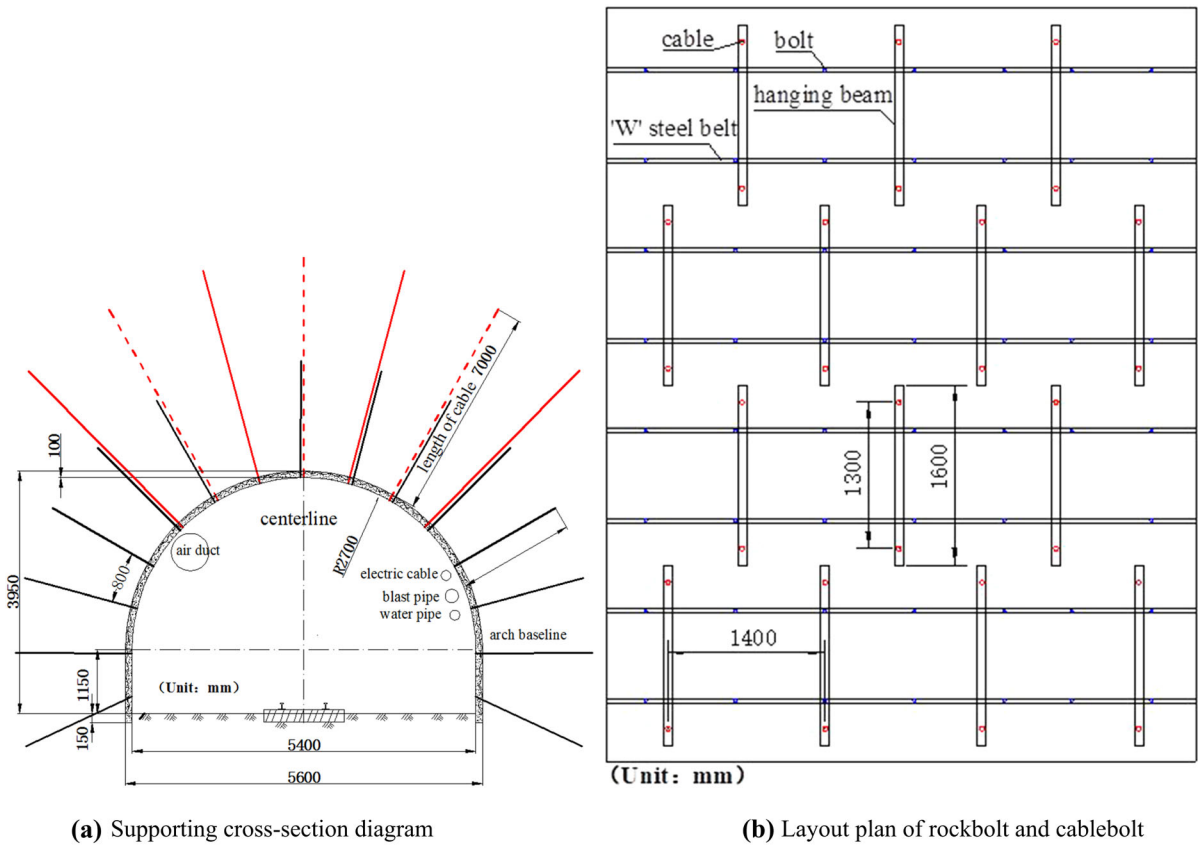


**Fig. 2** Original support scheme of roadway

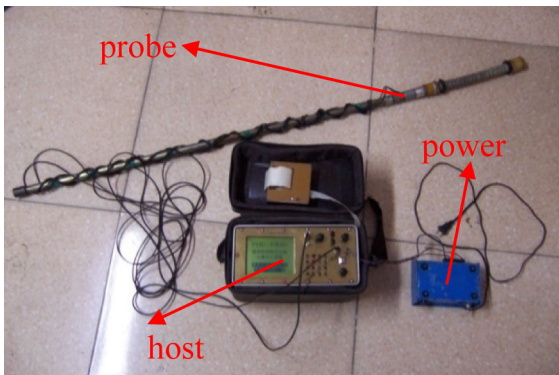


**Fig. 3** Ultrasonic instrument

The maximum anchoring force provided by rockbolt relates to withdrawal resistance of rockbolt, bearing capacity of face plate, resistance to extrusion of the screw thread, strength of anchorage, and take the minimum of the above values (Cai et al. 2004). The first three are related to the performance of rockbolt

and its related components. The strength of the anchorage is not only related to the surface shape of rockbolt and drill hole, the strength of resin, but also related to the strength of surrounding rock. These factors affecting the anchoring force can be controlled artificially in addition to that of surrounding rock, so the strength of surrounding rock become the uncontrollable factor to provide the maximum anchoring force under the same conditions.

The bonding interface fails when its shear stress reaches to the shear strength. The relationship between the strength of surrounding rock and the load of rockbolt is studied by establishing the mechanical model of the anchorage system at the resin–rock interface. To simplify the calculation, it is assumed that the anchorage is a rigid body, the shear deformation between anchorage and surrounding rock is coordinated. The shear stress at the interface is  $\tau(u)$ , where  $u$  is the shear displacement of the interface. The sketch of the anchorage element is shown in Fig. 11.

**Fig. 4** Layout of monitoring points

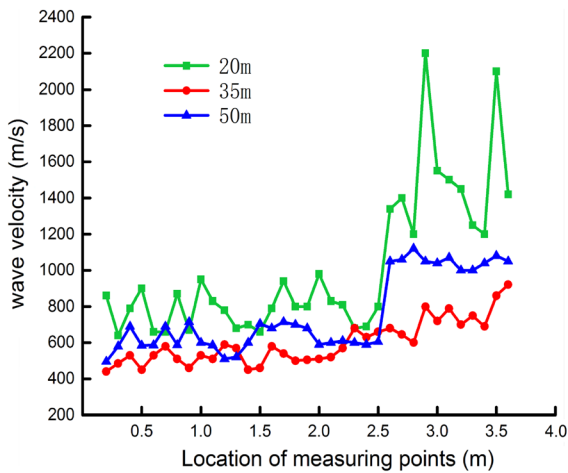
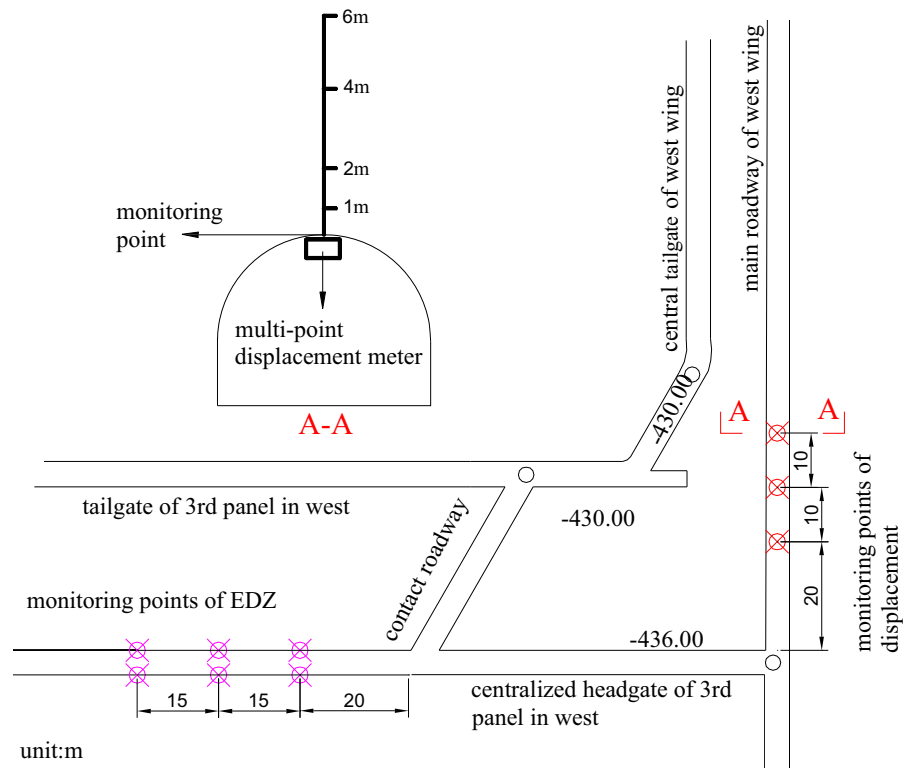


**Fig. 5** The wave velocity of left side of sidewall

According to the static equilibrium condition of the anchorage element, the following formula is obtained

$$\frac{du(x)}{dx} = -\frac{p(x)}{\pi r^2 E_0} \quad (1)$$

where,  $E_0$  is the equivalent elastic modulus of anchorage, its calculation method is given by

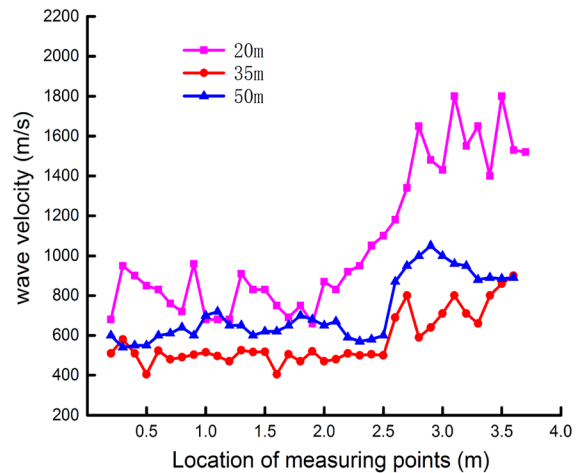


**Fig. 6** The wave velocity of right side of sidewall

$$E_0 = \frac{E_a A_1 + E_b A_2}{A_1 + A_2} = \frac{E_a (r_a^2 - r_b^2) - E_b r_b^2}{r_a^2} \quad (2)$$

where,  $A_1$  and  $A_2$  are cross-sectional area of resin and rockbolt, respectively;  $r_a$  and  $r_b$  are the radius of anchorage and rockbolt, respectively;  $E_a$  and  $E_b$  are the elastic modulus of resin and rockbolt, respectively.

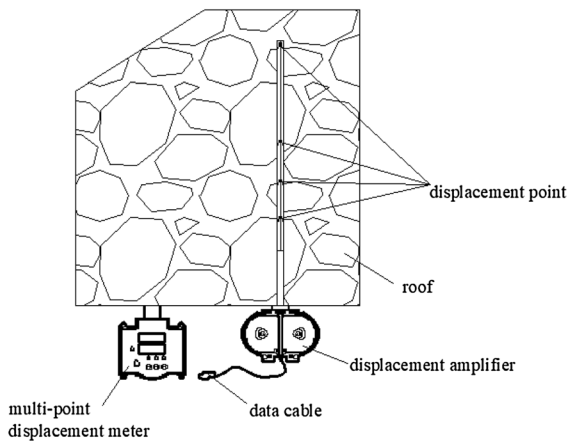


**Fig. 7** Sketch of multi-point displacement meter

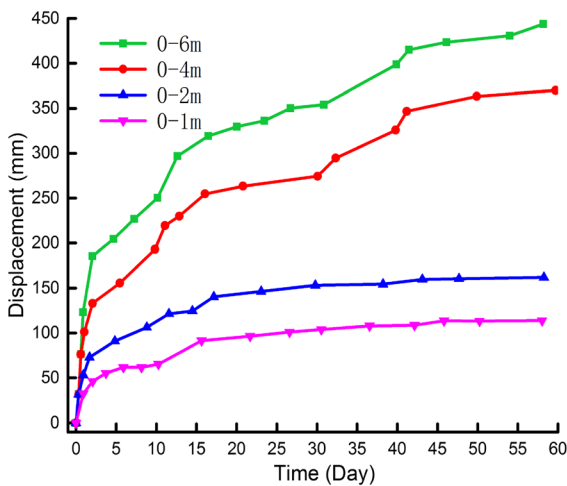


**Fig. 8** Displacement of monitoring point at 20 m

Taking the  $x$ -axis of the anchorage element as the projection axis, and analyzing equilibrium equation of force  $\sum Fx = 0$  can get

$$dP(x) = -2\pi r_a \tau(x) dx \tag{3}$$

The equilibrium differential equation of load transfer method of anchorage is obtained by Eqs. (1, 2, 3)

$$\frac{d^2 u(x)}{dx^2} = \frac{\tau(u)}{r_a E_0} \tag{4}$$

Assuming that the bonding interface is an incomplete elastic state, the linear load transfer function is given by

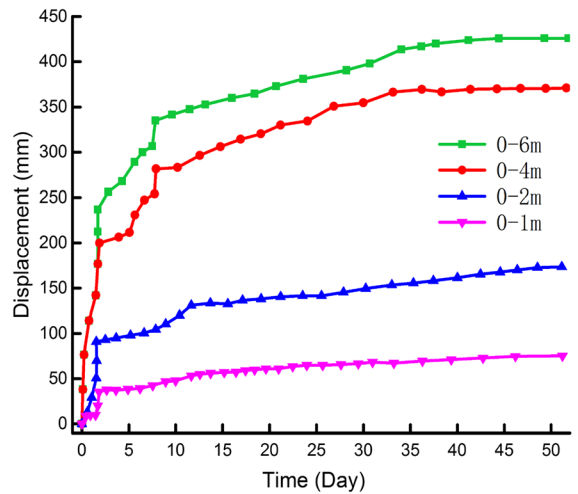


**Fig. 9** Displacement of monitoring point at 30 m

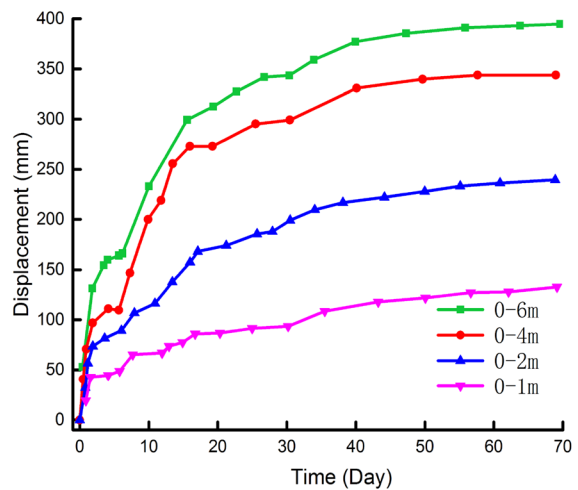


**Fig. 10** Displacement of monitoring point at 40 m

$$\tau(u) = ku \tag{5}$$

where,  $k$  is shear deformation rigidity between anchorage and surrounding rock.

The Eq. (5) is substituted into Eq. (4) to obtain the following equation

$$\frac{d^2 u}{dx^2} - \frac{ku}{r_a E_0} = 0 \tag{6}$$

Load of rockbolt is given by solving Eq. (6), which is substituted into boundary conditions  $P|_{x=0} = P$ ,  $P|_{x=L} = 0$ :

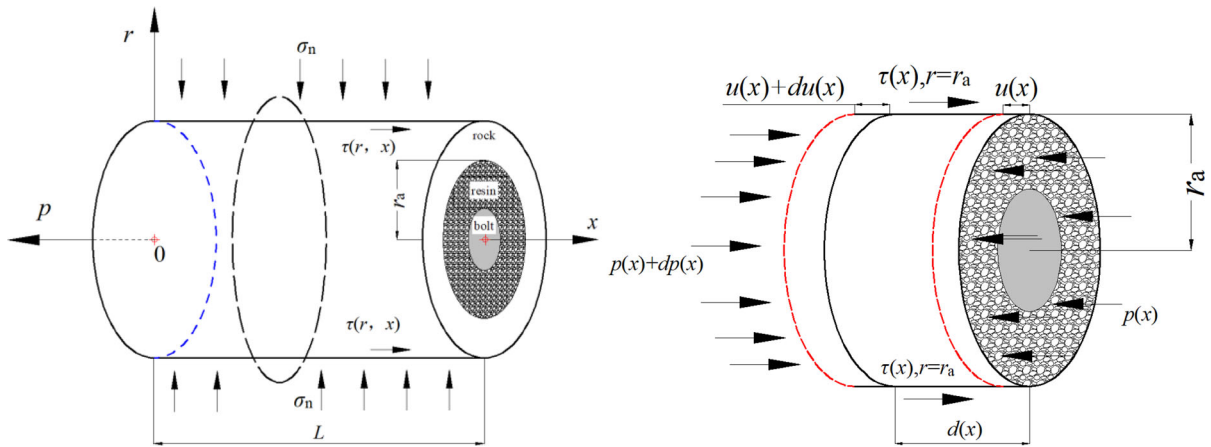


**Fig. 11** Sketch of uncoupled deformation between resin and surrounding rock

$$P(x) = \frac{p \cdot \sinh \left[ \sqrt{\frac{k}{r_a E_0}} (L - x) \right]}{\sinh \left( \sqrt{\frac{k}{r_a E_0}} L \right)} \tag{7}$$

Accordingly, the shear stress at the resin–rock interface is given by the following expression

$$\tau(x) = \frac{\sqrt{\frac{k}{r_a E_0}} \cosh \left( \sqrt{\frac{k}{r_a E_0}} (L - x) \right)}{\pi r_a \sinh \left( \sqrt{\frac{k}{r_a E_0}} L \right)} \tag{8}$$

Equations (7) and (8) are simplified formulas for anchorage in an elastic state. When the shear stress of anchorage interface reaches to its critical shear strength  $\tau_0$  in the position of  $x = 0$ , the critical pullout force  $P_0$  of anchorage is given by the following equation

$$P_0 = \frac{\pi r \tau_0 \tanh \left( \sqrt{\frac{k}{r_a E_0}} L \right)}{\sqrt{\frac{k}{r_a E_0}}} \tag{9}$$

From the Eq. (9), it is concluded that the critical shear strength of the resin–rock interface determines the maximum anchorage force  $P_0$  provided by rockbolt. Therefore, the larger the critical shear strength, the larger the anchoring force. The stress of surrounding rock redistributes after excavation. The surrounding rock, whose stress exceeds its critical strength, will yield and change from elastic zone to EDZ. The critical shear strength of EDZ belongs to the residual shear strength  $\tau_s$ , which is less than critical shear strength  $\tau_0$ . To achieve full performance of rockbolt materials, the maximum anchoring force provided by

anchorage should be greater than the breaking load of rockbolt, that is, the breaking failure of rockbolt occurs before the anchorage failure. For the type of partially-gouted, the anchoring force provided by the anchorage cannot reach to its design value if the anchorage is located in EDZ. In this case, the anchorage failure may occur before the breaking failure of rockbolt, that is, the rockbolt may be pulled out from anchorage rather than breaking, which causes the material performance of rockbolt cannot be fully utilized. Therefore, the anchorage should be located in a relatively stable elastic zone beyond EDZ.

The anchorage is located in elastic zone, the load in the non-anchorage section of rockbolt increases linearly with the increasing of deformation of surrounding rock. In this case, the load reaches to the breaking load of rockbolt, it will cause the breaking failure of rockbolt. The creep behavior is obvious for large deformation roadway in weak rock, the deformation of surrounding rock is larger than that of general roadway, and the load of rockbolt increases quickly. Note that it is assumed that the deformation process described occurs immediately upon excavation. This is a reasonable approximation for most roadways in rock. The effects of time dependent deformations upon the performance of the roadway and the design of the bolting system will be not be discussed in this paper. The key problem for roadway with high stress is to prevent the rockbolt from breaking prematurely. The solution is to prevent overload of rockbolt by setting the overload protection of rockbolt.

The shear strength of resin–rock interface is smaller than that of resin–bolt, the case in which the anchoring force of rockbolt will depend on the shear strength of resin–rock interface. The calculation of critical load-bearing capacity of rockbolt is usually given by the formula:

$$P_u = 2\pi r_a L \tau_0 \quad (10)$$

where,  $P_u$  is critical load-bearing capacity;  $L$  is the anchorage length;  $\tau_0$  the shear strength of resin–bolt interface. It can be seen from the formula (10) that the factors affecting the critical load-bearing capacity are borehole diameter, anchorage length, shear strength of resin–rock interface. The borehole diameter and anchorage length can be controlled artificially, while the shear strength  $\tau_0$  is related to the mechanical property of rock, which cannot be controlled artificially. Therefore, the weak rock will weaken the critical load-bearing capacity of rockbolt.

In summary, the anchorage is designed at the elastic zone, which can give full play to the material performance of rockbolt. However, with the expansion of EDZ, it will cause sliding failure of anchorage or breaking failure of rockbolt, and then results in bolting lifetime shorter, the cases in which are unfavorable for the stability control of surrounding rock and increases the number of repairs of roadway. It is necessary to adopt the reasonable bolting scheme to control the deformation of surrounding rock. Achieving full performance of rockbolt materials, lengthening the lifetime of rockbolt and maintaining the stabilization of roadway need to meet two criteria: the load of rockbolt does not exceed its critical breaking load; meanwhile, the anchorage should be located in the elastic zone beyond EDZ.

#### 4 Analysis of Irregular Deformation of Roadway

After understanding the failure type of bolting and the reasonable location of anchorage, it is very important to master the shape of EDZ to guide the correct bolting design. In the early stage of research, the shape of EDZ is mainly circular, elliptical and natural caving arch, which is suitable for the bidirectional isotropic rock, loose rock, and shallow depth rock. For underground rock, except for the deep strata of the earth's crust, most of the three-dimensional stress fields are not isotropic in three directions, and the magnitude and direction of its three principal stresses vary with space

and time, forming a specific four-dimensional stress field (Carranza-Torres and Fairhurst 2000). To effectively keep the stability of surrounding rock, it is necessary to study the development of EDZ under the condition of bidirectional anisotropic, and to seek the scientific and reasonable supporting measures.

##### 4.1 Boundary Equation of EDZ

EDZ is quite universal in rock at depth, where redistributed stresses are high compared with rock strength. In order to generate analytical solutions to more complicated rock mechanics problems, it does, however, demand several rather over-simplified assumptions, namely that the strata are isotropic, homogeneous and originally elastic, that the roadway is circular and deforms under plane strain conditions, that body forces approximate to zero and that the stress field is hydrostatic. It is not taken into account the bed separation of rock in solving EDZ, the purpose of which is to have a clear grasp the EDZ development law and the relationship with loading, to find the reason why only some rockbolts or cablebolts fail, to put forward the correct bolting principle. Therefore, provided that the surrounding rock is homogeneous and isotropic, the in-situ stress in horizontal and vertical directions is constant along the length direction of the roadway. In the case, the plane strain problem can be used to take any cross-section of roadway as a representative to study. The radius of roadway is  $R_0$ , that of the EDZ is  $R_p$ , the buried depth of roadway is more than  $20 R_0$ , in which the error compared with the original problem is not more than 5% if ignoring the effects of rock weight of influence range ( $5 R_0$ ) around the roadway. Therefore, the in-situ stress in the horizontal direction can be simplified as uniform distribution, for the case in which the actual roadway model can be simplified as a circular hole problem in plane strain with axial symmetry of load.

For the case that the angle between the direction of horizontal stress and the horizontal plane is 0, the mechanical model is shown in Fig. 12. In answer to this problem, the Kirsch equation (Jaeger et al. 2007), which is now well known, has been derived in the literature of Jaeger and Cook, that is no longer repeated here. The formulas are expressed in the form of polar coordinates, and the stresses at any point in the model can be determined by  $r$  and  $\theta$ .



$$\begin{aligned}
 f(r, \theta) = & \left\{ P_1(\lambda + 1)(R_0^2/r^2) - P_1(\lambda - 1) \cos 2\theta \left[ 1 + 3(R_0^2/r^2)^2 - 2(R_0^2/r^2) \right] \right\}^2 \\
 & + \left\{ P_1(\lambda - 1) \sin 2\theta \left[ 1 - 3(R_0^2/r^2)^2 + 2(R_0^2/r^2) \right] \right\}^2 \\
 & - \frac{(1 - \cos 2\varphi)}{2} \left\{ [P_1(\lambda + 1) - 2 \cos 2\theta (R_0^2/r^2) P_1(\lambda - 1)]^2 - 4c^2 \right\} \\
 & - 2c \sin 2\varphi [P_1(\lambda + 1) - 2(R_0^2/r^2) P_1(\lambda - 1) \cos 2\theta] - 4c^2
 \end{aligned}
 \tag{11}$$

Traditional approaches of modeling rock failure employ the linear Mohr–Coulomb failure criterion, based on which the implicit equation of EDZ of the circular roadway is given by

where,  $\lambda$  is lateral pressure coefficient, which is the ratio of horizontal load to vertical load;  $P_1$  is vertical load;  $c$  is cohesion of model;  $\varphi$  is angle of friction.

The boundary equation between elastic zone and EDZ can be obtained when  $f(r, \theta) = 0$ , as shown in Fig. 13. The depth equation of EDZ under biaxial isotropic stress field can be solved if  $\lambda = 1.0$ ; if not, that under biaxial isotropic stress field can be solved. According to the Eq. (11), setting certain parameter values, for example,  $P_1 = 20$  MPa,  $R_0 = 2$  m,  $c = 3.0$  MPa,  $\varphi = 25^\circ$ . The influence of  $\lambda$  on the distribution of EDZ is studied by changing the  $\lambda$  value, from which it can be seen that the irregular shape of EDZ is more and more obvious, which develops gradually from circular to oval, finally into a ‘butterfly-shaped’ with  $\lambda < 1.0$  gradually. The EDZ in shoulder of roadway is greater than that in top, bottom

and two sidewalls. When the in-situ stress direction is inclined or changed due to the influence of mining disturbance, the shape of EDZ will deflect accordingly. The mechanical model of the roadway, is shown in Fig. 14 when the in-situ stress direction rotates  $25^\circ$ . According to the Eq. (11), the corresponding EDZ shape is obtained by adjusting the stress direction, as shown in Fig. 15.

In summary, the depth of EDZ at each radial direction of roadway is not only related to the lateral pressure coefficient but also related to the stress direction of in-situ stress. The lateral pressure coefficient affects the shape of EDZ, while the stress direction of in-situ stress affects the deflection angle of EDZ. At present, the roadway is basically in the anisotropic stress field, which makes the depth of EDZ at each radial direction of roadway different. At present, the bolting design adopts the idea of uniform

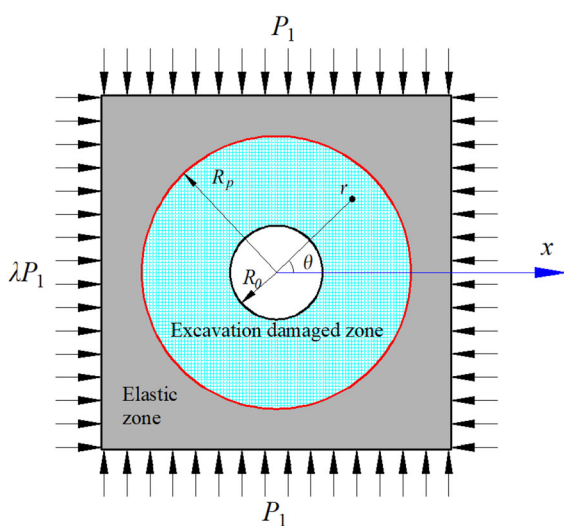


Fig. 12 Mechanical model of roadway

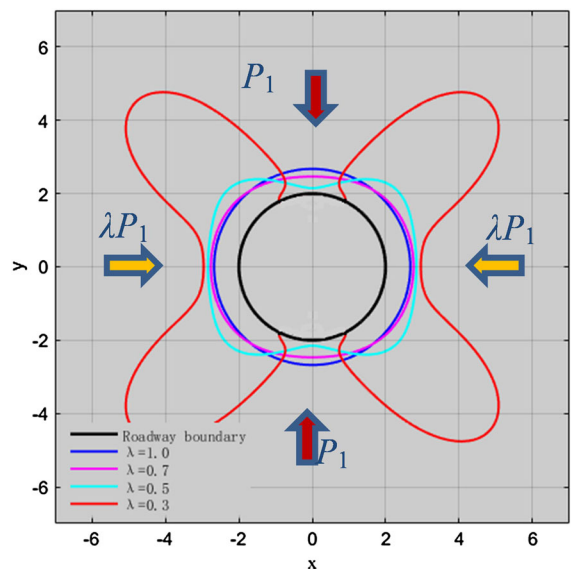
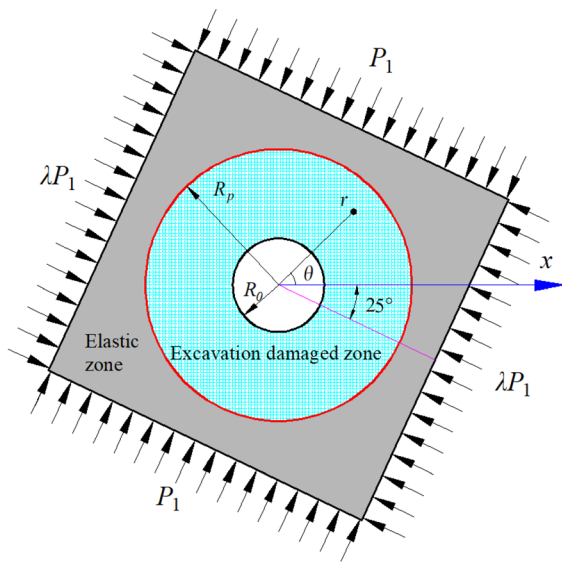
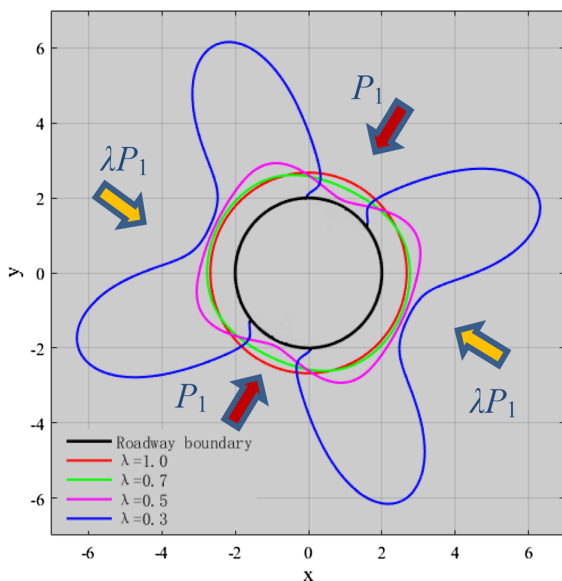


Fig. 13 EDZ shape of roadway under horizontal stress condition



**Fig. 14** In-situ stress rotates 25°



**Fig. 15** The shape of EDZ rotated 25°

supporting strength for the full cross-section, the value of which based on the weakest strength of surrounding rock. This bolting method is not only easy to bring about excessive support in some parts of surrounding rock but also to lead to the insufficient support on other parts of surrounding rock. The reasonable bolting design should adopt the principle of coordinated support based on the depth of EDZ at different radial positions, that is, the position of anchorage should be

located in the elastic zone. For the convenience of narration, this paper only discusses the situation of circular roadway, but these principles apply to any shape of roadway.

#### 4.2 Techniques for Controlling EDZ

If  $\lambda = 1.0$ , the roadway is in the stress state of bidirectional isotropic. By comparing the stress distribution between the elastic state and elastic–inelastic state, it is due to the existence of EDZ that the minimum principal stress increases and the maximum principal stress decreases, which give rise to the surrounding rock to be destroyed difficultly. The case indicates that the EDZ plays a supporting role on the surrounding rock in the elastic zone.

Provided the rock in EDZ is taken out, the roadway radius will increase, and leads to the stress redistributed again, resulting in the new EDZ. Therefore, the way to prevent the radius of roadway from increasing indirectly by maintaining the rock in EDZ can effectively improve stress state of surrounding rock outside the EDZ. Meanwhile, the existence of EDZ provides certain confining pressure to surrounding rock outside the EDZ, which is conducive to the maintenance of roadway. There is a positive correlation between the deformation of surrounding rock and the depth of EDZ, which can conclude that the key to controlling the deformation of surrounding rock is to control the depth of EDZ.

If the supporting strength provided by rockbolts can make the stress state of surrounding rock reach to the in-situ stress state, the EDZ would not expand outwards. However, due to the limitation of material and construction technology, the rockbolts cannot provide the supporting strength in the same order of magnitude with the in-situ stress. As a result, it is difficult to change the evolution process of the stress field in surrounding rock for relatively small supporting strength, and it cannot change the fact that the EDZ in the weak rock continues to expand outwards. At present, the best way is to reduce the expansion rate of EDZ by the reasonable bolting scheme. The residual strength of broken rock inside EDZ is lower, which is basically in the same order of magnitude with supporting resistance provided by the pre-stressed rockbolts. Although the high pre-stress of rockbolts have little effect on improving the peak strength of surrounding rock, it can effectively improve the

residual strength of rock and form a larger area of effective compressive stress in the roof, which can give full play to the active support function of rockbolts (Kang et al. 2009; Wang et al. 2016;). Therefore, the effective way to control EDZ expansion of surrounding rock is to enhance the active support function of rockbolts by installing the rockbolts with high pre-stress, in order to increase the residual strength of broken rock to control its fractured swelling deformation. Using the above methods, the expansion rate of EDZ can be controlled indirectly.

## 5 Engineering Application Example

### 5.1 The Design of Support Scheme

To solve the problem that the rockbolts are often pulled out and the cablebolts are broken easily, the bolting design should follow the analysis of the previous anchorage and control principle of EDZ, and adopt the coordinated support design according to the depth of EDZ. It can be seen from the above analysis of monitoring data that, the pullout failure is due to the insufficient length of rockbolt, which causes the anchorage to be located in EDZ, while the reason of cablebolt breaking failure is that the elongation of cablebolt is so insufficient that cannot adapt to the large deformation of surrounding rock. Therefore, the authors put forward a new bolting technology instead of combined support with rockbolt and cablebolt.

The combination rockbolt is the rockbolt which can be lengthened by couplers, which allow one to put tension in the rockbolt by mechanically pulling the non-encapsulated bottom against the resin encapsulated top. The top anchor is provided by a resin column around the rebar and the lower anchor by the face plate against the roofline. The combination rockbolt is made of ribbed bar with non-longitudinal ribs. Its elongation

is more than 15%, its yield strength is more than 335 Mpa, its tensile strength is more than 490 Mpa.

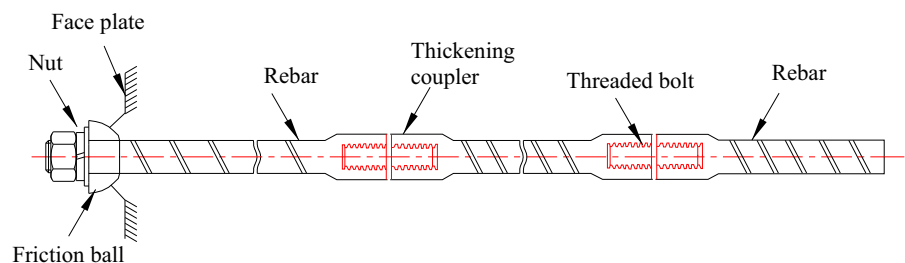
The combination rockbolt (Fig. 16) can set the number of connecting rockbolts according to the depth of EDZ to make the anchorage placed in the stable elastic zone. It can solve the problem that the ordinary long rockbolt can't be used because of the lack of roadway space. And the combination rockbolt has more reasonable extension characteristics than cablebolt. It is not easy to break and can provide high anchoring force continuously in the process of deformation due to the function of "high-resistance and pressure-relief". Therefore, the combination rockbolt provides a new means for roadway with large deformation.

For the rockbolt with diameter 20 mm, the diameter of the thickening connector is 5 mm larger than that of threaded rockbolt. The diameter of the connection head is  $25 \pm 5$  mm. The length of the connection head is 50 mm. The specification of connection rockbolt is M18. The arc transition zone and threaded rockbolt at the joint are still the weak of the whole system after all. To improve the reliability of the system, radian optimization in the joint between threaded rockbolt and thickening connector is done, so the stress in the joint is more uniform, its strength is matched with that of the threaded rockbolt. The dimension of the joint is shown in Fig. 17.

The compressive strength of the selected capsule resin is more than 60 Mpa, its anchoring force is more than 125 kN. There is no corrosion effect on rockbolt and there is a good impermeability. The borehole diameter is 28 mm.

In order to compare the mechanical properties between the combination rockbolt and ordinary rockbolt and cablebolt, the pull-out testing of the original rockbolt  $\Phi 20 \text{ mm} \times 2000 \text{ mm}$ , the pre-stressed cablebolt  $\Phi 17.8 \text{ mm} \times 4000 \text{ mm}$  and the combination rockbolt  $\Phi 20 \text{ mm} \times 4000 \text{ mm}$  were carried out

**Fig. 16** Sketch of combination rockbolt



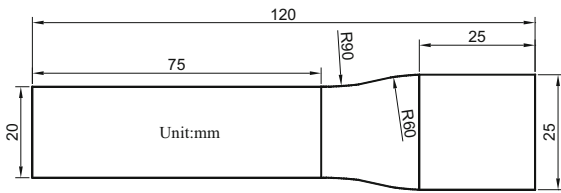


**Fig. 17** Optimized size of rockbolt's joint

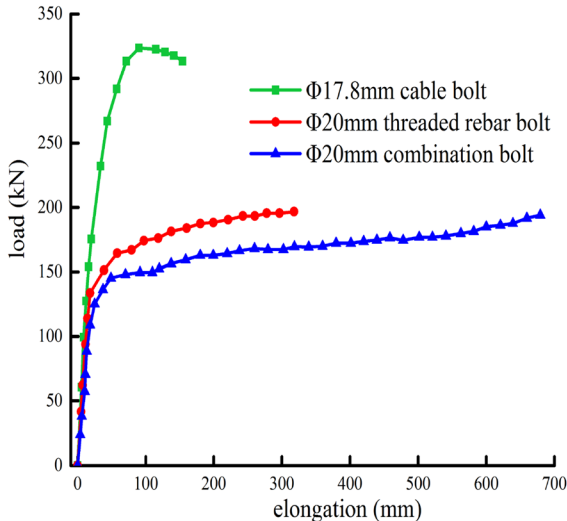


**Fig. 18** Tensile test curve of rockbolt (cablebolt)

in laboratory, which obtained the corresponding relationship between their load and elongation (Fig. 18).

Through the analysis of pull-out testing results, the maximum load of combination rockbolt is 183 kN, whose extension is 685 mm, and the elongation is about 17%, which is much higher than the elongation rate of the ordinary rockbolt, only 3%. The combination rockbolt can still maintain a higher load (about 150 kN) after the extension reached to 135 mm, and the load would be stable at 170–180 kN with its extension. The mechanical properties of the combination rockbolt ensure that it still is not broken after a certain deformation, and bears high load continuously. Although the tensile strengths of the rockbolt with 20 mm and 17.8 mm diameter are up to 200 kN and 355 kN respectively, the breaking failure occurs when their extensions are only 310 mm and 120 mm.

Combined with the control principle of EDZ earlier in the article, the design of bolting scheme for the main roadway of Puhe Coal Mine is carried out by using the combination rockbolt. The bolting scheme is as

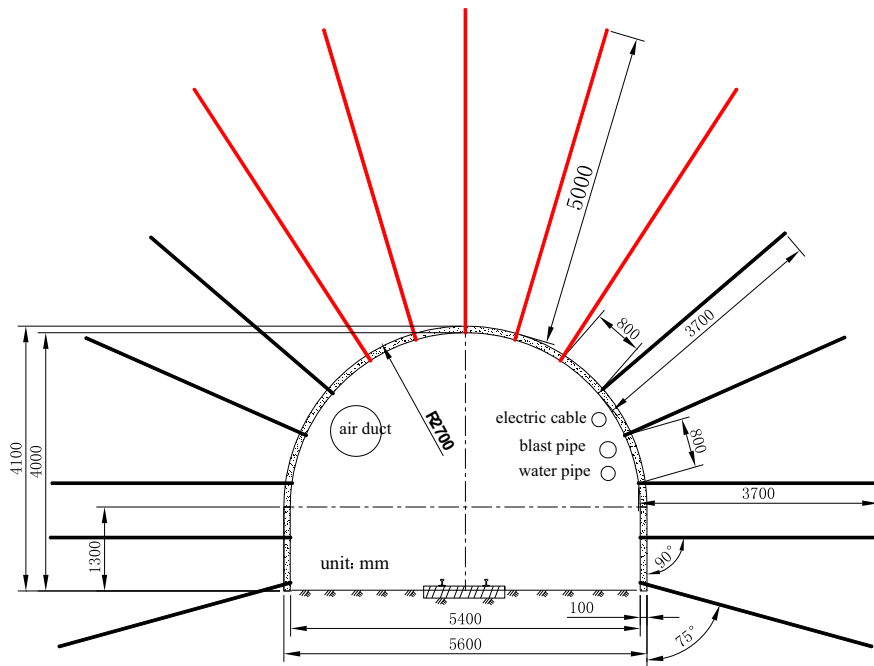
follows: The two sidewalls and arch shoulder are supported by  $\Phi 20 \times 3700$  mm combination rockbolt composed of two rockbolts which is 1200 mm length and 2500 mm length respectively. The vault is supported by combination rockbolt of  $\Phi 20 \times 5000$  mm made up of two rockbolts of 2500 mm length. All the row spacing between the rockbolts are  $800 \times 800$  mm, and the type of partially-grouted was adopted. The anchorage length is 1500 mm with three capsule resins, 500 mm length. The bolting parameters are shown in Fig. 19.

## 5.2 Analysis of Bolting Effect

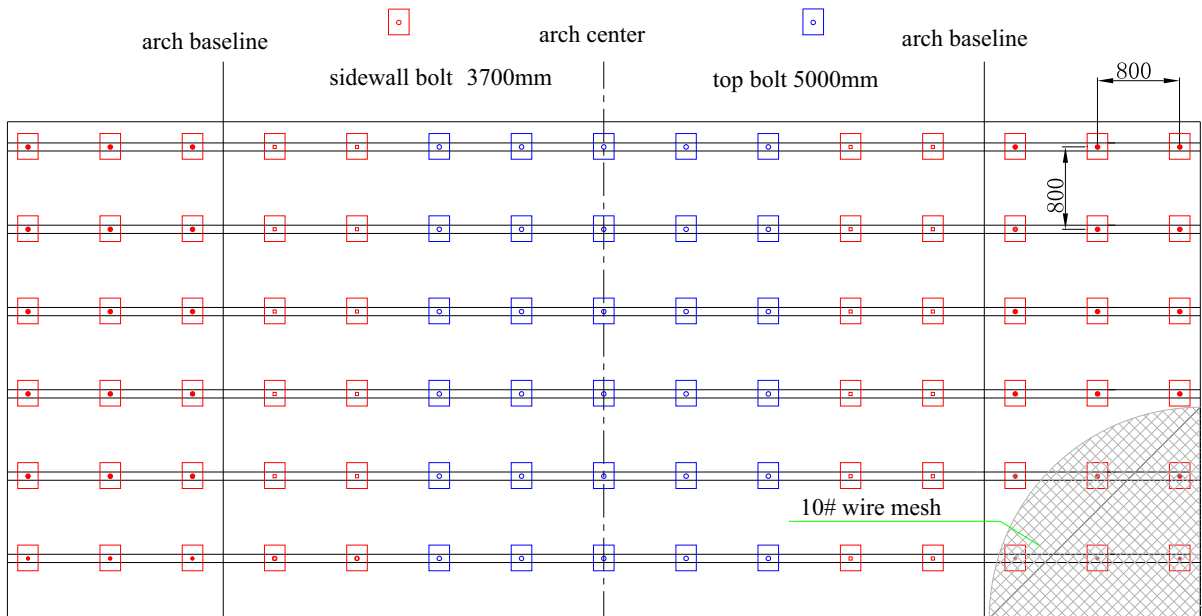
It is necessary to observe the rock stress to understand the convergence between two sidewalls, the displacement and bed separation of surrounding rock, rockbolt and cablebolt stress and so on after the new bolting scheme is adopted. These observations can determine whether the bolting scheme are reasonable and can provide a basis for the optimization of scheme. The test roadway was arranged three displacement and anchoring force monitoring points for combination rockbolts, respectively.

The monitoring data in Figs. 20 and 21 show that the deformation rate and deformation of surrounding rock both are larger during 25 days. The maximum convergence between two sidewalls was about 90 mm, and the maximum displacement of roof was about 175 mm, after which the deformation rate decreases. On the 80th day, the maximum convergence was about 119 mm, and that of roof displacement was about 205 mm, which can be reduced by more than 50% compared with the displacement of original bolting scheme and which was less than the maximum extension of the combination rockbolt. The rockbolts were in stable working state. Although the surrounding rock has been in a continuous state of deformation, its deformation rate is low, which can meet the requirements for safety production. No breakage failure, pull-out failure of the rockbolts have been found during the period of production, which reduces the maintenance cost and essentially changes the support condition of roadway.

The monitoring data in Figs. 22, 23 and 24 show that the changes of anchoring force of 5 m combination rockbolts have the same trend with that of 3 m combination rockbolts. The growth rate is high in the initial stage, after which it slows down and there is a



(a) bolting scheme of section



(b) Inter-row spacing layout of rockbolts

**Fig. 19** Combination rockbolt support scheme

significant fluctuation of anchoring force. The fluctuation of some rockbolts is great due to the complex

geological conditions of Puhe Coal Mine, which is not avoided deliberately in the choice of test roadway in

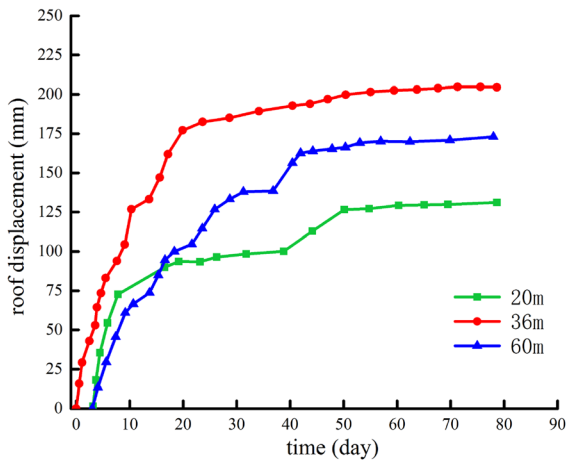


**Fig. 20** Roof displacement

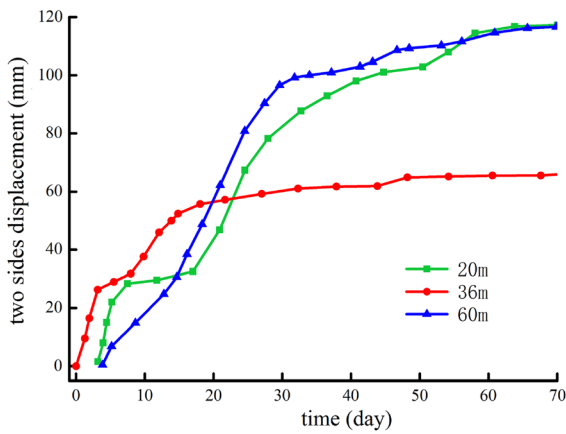


**Fig. 21** Convergence between two sidewalls

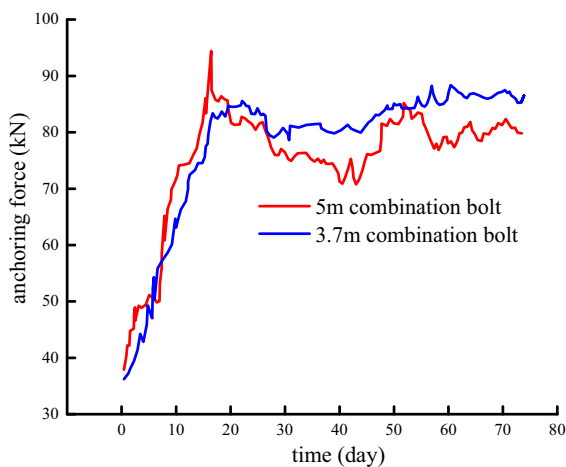


**Fig. 22** Anchoring force at station 1

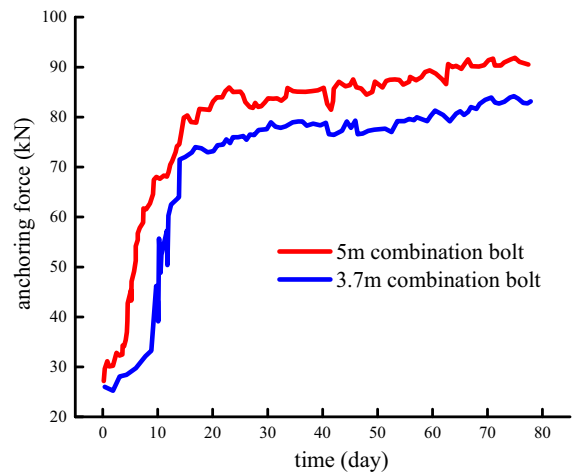


**Fig. 23** Anchoring force at station 2

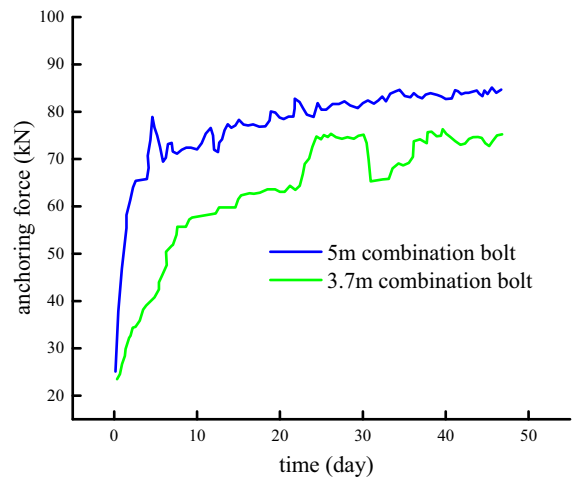


**Fig. 24** Anchoring force at station 3

order to test the supporting effect of combination rockbolts. The anchoring force of rockbolts is maintained between 70 and 100 kN, the case in which illustrates that the combination rockbolts work well and have played a supporting role in surrounding rock.

### 6 Conclusions

A mechanical model for anchorage and surrounding rock is established, the following conclusions are obtained by solving the differential equation of load transfer. Two conditions must be met to achieve full performance of rockbolt materials and to lengthen the service life of rockbolt, one is that the load of rockbolt

is not more than its load-bearing load, the other is that the anchorage should be located in stable elastic zone, which is located outside EDZ of surrounding rock.

The shape of EDZ is closely related to the lateral pressure coefficient. If the lateral pressure coefficient is  $\lambda = 1.0$ , the shape of EDZ is circular; if not, it is irregular, and the larger the degree of lateral pressure coefficient deviates from 1.0, the more obvious the irregular shape is. The shape of EDZ rotates with the change of the direction of in-situ stress. The reasonable bolting design should adopt the principle of coordinated support based on the depth of EDZ at different radial positions of roadway, that is, the position of anchorage should be located in the elastic zone to avoid excessive support in some parts of surrounding rock and to avoid bolting failure.

The combination rockbolt is a new type of rockbolt which can set the length according to the depth of the EDZ. And it can solve the problem that the ordinary long rockbolt can't be used because of the lack of roadway space, can ensure anchorage to be located in the stable elastic zone, and can solve the problem that the cablebolt can not meet the large deformation of weak rock due to its small elongation. The combination rockbolt scheme successfully solves the problem of the main roadway Puhe Coal Mine that the rockbolt is often pulled out and the cablebolt breaks easily, meanwhile, controls the deformation of surrounding rock well and obtains a good economic benefit.

**Acknowledgements** This work was supported by the National Natural Science Foundation of China (Grant Nos. 51434006, 51874130); Research and innovation project of graduate students in Hunan Province (Grant No. CX2017B648).

#### Compliance with ethical standards

**Conflict of interest** No potential conflict of interest was reported by the authors.

#### References

- Anagnostou G, Perazzelli P (2015) Analysis method and design charts for bolt reinforcement of the tunnel face in cohesive-frictional soils. *Tunn Undergr Sp Tech* 47:162–181
- Barton N, Shen B (2016) Risk of shear failure and extensional failure around over-stressed excavations in brittle rock *J Rock Mech. Geotech Eng* 9(2):210–225
- Blanco Martín L, Tijani M, Hadj-Hassen F et al (2013) Assessment of the bolt-grout interface behaviour of fully grouted rockbolts from laboratory experiments under axial loads. *Int J Rock Mech Min* 63:50–61
- Cai Y, Esaki T, Jiang YJ (2004) A rock bolt and rock mass interaction model. *Int J Rock Mech Min Sci* 41:1055–1067
- Cai Y, Jiang YJ, Djamaluddin I et al (2015) An analytical model considering interaction behavior of grouted rock bolts for convergence–confinement method in tunneling design. *Int J Rock Mech Min* 76:112–126
- Carranza-Torres C, Fairhurst C (2000) Application of the convergence-confinement method of tunnel design to rock masses that satisfy the Hoek-Brown failure criterion. *Tunn Undergr Sp Technol Inc Trenchless Technol Res* 15:187–213
- Farmer I (1975) Stress distribution along a resin grouted rock anchor. *Int J Rock Mech Min Sci Geomech Abstr* 12:347–351
- Hyett AJ, Bawden WF, Macsporrán GR et al (1995) A constitutive law for bond failure of fully-grouted cable bolts using a modified hoek cell. *Int J Rock Mech Min Sci Geomech Abstr* 32:11–36
- Indraratna B, Kaiser PK (2010) Analytical model for the design of grouted rock bolt. *Int J Numer Anal Methods Geomech* 14:227–251
- Jaeger JC, Cook NGW, Zimmerman RW (2007) *Fundamentals of rock mechanics*. Blackwell Publishing, Hoboken
- Kang HP, Lin L, Wu YZ (2009) Development of high pretensioned and intensive supporting system and its application in coal mine roadways. *Proc Earth Planet Sci* 1(1):479–485
- Kilic Y, Celik AG (2002) Effect of grout properties on the pull-out load capacity of fully grouted rock bolt. *Tunn Undergr Sp Technol Inc Trenchless Technol Res* 17:355–362
- Li D, Masoumi H, Hagan PC et al (2019) Experimental and analytical study on the mechanical behaviour of cable bolts subjected to axial loading and constant normal stiffness. *Int J Rock Mech Min* 113:83–91
- Li D, Masoumi H, Saydam S et al (2017) A constitutive model for load-displacement performance of modified cable bolts. *Tunn Undergr Sp Tech* 68:95–105
- Li C, Stillborg B (1999) Analytical models for rock bolts. *Int J Rock Mech Min* 36:1013–1029
- Li L, Hagan PC, Saydam S et al (2019) A laboratory study of shear behaviour of rockbolts under dynamic loading based on the drop test using a double shear system. *Rock Mech Rock Eng*. <https://doi.org/10.1007/s00603-019-01776-x>
- Peila D (1994) A theoretical study of reinforcement influence on the stability of a tunnel face. *Geotech Geol Eng* 12:145–168
- Serrano A, Olalla C (1999) Tensile resistance of rock anchors. *Int J Rock Mech Min Sci* 36:449–474
- Tahmasebinia F, Zhang C, Canbulat I et al (2018) Numerical and analytical simulation of the structural behaviour of fully grouted cable bolts under impulsive loading. *Int J Min Sci Technol* 28:807–811
- Teymen A, Kılıç A (2018) Effect of grout strength on the stress distribution (tensile) of fully-grouted rockbolts. *Tunn Undergr Sp Tech* 77:280–287
- Tsang C, Bernier F, Davies C (2005) Geohydronechanical processes in the excavation damaged zone in crystalline rock, rock salt, and indurated and plastic clays-in the context of radioactive waste disposal. *Int J Rock Mech Min* 42:109–125

- Wang H, Jiang Y, Xue S, Shen B, Wang C, Lv J, Yang T (2015) Assessment of excavation damaged zone around roadways under dynamic pressure induced by an active mining process. *Int J Rock Mech Min* 77:265–277
- Wang Q, Pan R, Jiang B et al (2017) Study on failure mechanism of roadway with soft rock in deep coal mine and confined concrete support system. *Eng Fail Anal* 81:155–177
- Wang WJ, Yuan C, Yu WJ et al (2016) Stability control method of surrounding rock in deep roadway with large deformation. *J China Coal Soc* 41(12):2921–2931
- You CA, Zhan YB (2005) Distributing characters and analysis of stresses in prestressed cables. *Chin J Rock Mech Eng* 24(6):925–928
- Yu S, Zhu W, Niu L et al (2019) Experimental and numerical analysis of fully grouted long rockbolt load-transfer behavior. *Tunn Undergr Sp Tech* 85:56–66
- Zou JF, Zhang PH (2019) Analytical model of fully grouted bolts in pull-out tests and in situ rock masses. *Int J Rock Mech Min* 113:278–294

**Publisher's Note** Springer Nature remains neutral with regard to jurisdictional claims in published maps and institutional affiliations.